

Damage Evolution Formulation: A New Approach

Rute Lemos^{a*}, Ana Mendonça^{ab}, Conceição J.E.M. Fortes^a, Carolina Martinez^a, Helder Girão^b, Tiago Lopes^b, Lucas Brito^c, Nuno Lopes^c, Ana Prior^c

^aLNEC - National Laboratory for Civil Engineering, Lisbon, Portugal

^bISEC - Instituto Superior de Educação e Ciências, Lisbon, Portugal

^cISEL - Instituto Superior de Engenharia de Lisboa, Lisbon, Portugal

* Corresponding author: Address: LNEC, Avenida do Brasil 101, 1700-066 Lisboa, Portugal; email: rlemos@lnec.pt

ABSTRACT: One of the most influential contributions to damage progression formulations was introduced by Melby and Kobayashi. Their initial model was published in Melby and Kobayashi (1988a, b) and subsequently reformulated in Melby and Kobayashi (1999) to allow for non-zero initial damage values. A comprehensive description of these developments is provided in Melby (1999). The formulation predicts damage evolution in rubble mound breakwaters (RMBs) with rock-armoured layers, based on erosion measured in physical scale-model tests and on the characteristics of the incident wave conditions. However, the applicability of this formulation is limited to rock armour layers and to the range of sea states investigated in the original experiments. The present work revisits the Melby and Kobayashi damage evolution formulation and investigates its extension to rubble mound breakwaters armoured with tetrapods. A first approach was previously undertaken using a two-dimensional scale model of a section of the Ericeira breakwater (Lemos et al., 2023), leading to the calibration of new coefficients for the Melby formulation ($a_p = 0.03$ and $b = 0.16$). The objective of the present study is to further adjust these coefficients for comparable sea states while accounting for three-dimensional effects on damage evolution, including frontal wave attack. To this end, a long-duration test series (Series A) and two additional series with limited test durations (Series B and C) were conducted using a 1:65 three-dimensional physical model of the Ericeira harbour breakwater. The eroded volume of a selected section of the armour layer was measured using a Kinect position sensor. The damage parameter values obtained from the three-dimensional experiments are higher than those predicted by the formulation derived from the two-dimensional tests (Lemos et al., 2023). Based on the three-dimensional experimental results, new values of the coefficients a_p and b for the Melby and Kobayashi formulation were determined by minimising the root mean square error between measured and predicted damage. The predictive relationships proposed by Melby and Kobayashi (1988a, b), calibrated with $a_p = 0.025$ and $b = 0.30$ for the present test programme and accounting for three-dimensional effects associated with bathymetry, are shown to provide a reasonable description of damage evolution, with deviations remaining within an acceptable standard deviation.

1 INTRODUCTION

Rubble-mound breakwaters are the most common type of breakwaters in Portugal, being suitable for regions with severe wave conditions. They have an approximately trapezoidal cross-section, consisting of a core of stones covered by large rock armor or concrete blocks (Fig. 1). The progressive nature of their failure, mainly in the armour layer, is one of their characteristics, allowing for timely repairs.

Given the unpredictable nature of wave impacts on RMBs, the potential effects of climate change, the significant investment required for their construction, and their important role in safeguarding ports, it's essential to monitor the performance of RMBs regularly. This helps to identify maintenance and repair needs, avoiding higher risks or costs.



Figure 1. Breakwater armour layers composed of: (a, b) concrete units (Ericeira and Sines); (c) rock units (Vila Praia de Âncora)

The study of damage progression in rubble-mound breakwaters has advanced considerably over recent decades, driven by improvements in theoretical modelling, empirical research, and experimental techniques. Damage assessment in RMBs is influenced by factors such as structural geometry, design specifications, and the type of armour units employed. Damage is typically characterised by the degree of reshaping within the armour layer and is associated with the prevailing failure mode. Quantification may be based on the volume of eroded material or the number of displaced armour units (Campos et al., 2020).

To accurately evaluate breakwater stability, an appropriate damage descriptor must be selected. One widely used approach is displacement counting, in which damage (D) is related to different types of armour unit movement, including rocking. The number of displaced units is commonly normalised by the total number of units within a vertical strip of width equal to the nominal diameter (D_n), extending from the toe to the crest of the armour layer. Van der Meer (1988) introduced the parameters N_{od} (units displaced out of the armour layer) and N_{or} (rocking units); however, these parameters are limited by their dependence on slope length and strip geometry (CEM, 2011).

An alternative and widely adopted damage descriptor is the dimensionless damage parameter

$$S = \frac{A_e}{D_{n50}^2},$$

originally introduced by Broderick (1983), where A_e represents the eroded area and D_{n50} is the nominal median armour diameter.

Early insights into breakwater stability were provided by Hudson (1958), whose formula offered a basic static method for determining armour unit size as a function of wave height and structure slope. While foundational, Hudson's approach assumes a deterministic structural response and does not account for the progressive accumulation of damage, thereby limiting its applicability for long-term performance assessment under sustained wave loading.

A major advancement was achieved by Van der Meer (1988a), who proposed a semi-empirical model capable of capturing gradual damage accumulation due to repeated wave action. This approach incorporated key parameters such as wave height, wave period, and structural

permeability, with the damage parameter S serving as a central indicator of armour unit displacement. This marked a transition from static to dynamic damage assessment.

Further progress was made by Melby and Kobayashi (1999), who developed a wave-by-wave damage accumulation model that explicitly accounts for the stochastic and cumulative effects of individual wave impacts. Their formulation recognises that each wave contributes incrementally to structural deterioration. A comprehensive description of this methodology is provided in Melby (1999).

More recently, Lemos et al. (2023) conducted several test series using a two-dimensional physical scale model of a section of the Ericeira breakwater. Following the methodology proposed by Melby (1999), that study revisited the damage evolution formulations of Melby and Kobayashi and extended their applicability beyond rock armour layers by developing a predictive formulation for tetrapod armour units. Long-duration tests were performed using a 1:50 scale model of the quay section of the Ericeira Harbour breakwater, with eroded armour volumes measured using a Kinect position sensor. The measured damage values were lower than those predicted by formulations calibrated for rock armour, reflecting the smoother and slower damage progression typically observed in tetrapod armour layers.

Based on those results, new coefficients a_p and b for the Melby formulation were calibrated for the tested tetrapod armour layer by minimising the root mean square error between measured and predicted damage. The adjusted coefficients were $a_p = 0.030$ and $b = 0.16$.

The present study aims to further refine these empirical coefficients by conducting tests under comparable sea states using a three-dimensional physical scale model, thereby accounting for three-dimensional effects associated with bathymetry and wave attack. To this end, three test series were performed using a 1:65 three-dimensional scale model of the Ericeira Harbour breakwater. Although bathymetric changes in the vicinity of rubble-mound structures located in the surf zone can significantly influence damage evolution (Yuksel and Kobayashi, 2022), as is the case for the Ericeira breakwater, the present model was constructed on a fixed bottom. This represents a common simplification in stability

studies when sedimentological processes are not the primary focus.

In addition, three-dimensional surveys of the armour layer were conducted using a Kinect position sensor to characterise damage evolution with high spatial resolution.

Following this introduction, the Materials and Methods section describes the Melby-based methodology, the experimental setup, and the measurement procedures adopted in the physical model tests of the Ericeira breakwater. The experimental results are presented and discussed in Section 3, and the main conclusions of the study are summarised in Section 4.

2 MATERIALS AND METHODS

2.1 Formulae for Armour Layer Damage Evolution

Burcharth and Hughes 2011 explain that the stability of an armour layer can be assessed through the ratio between destabilising and stabilising forces. This ratio is expressed by the stability number N_s , a dimensionless indicator of armour stability that should be kept as low as possible to ensure a stable armour layer. Based on laboratory experiments, the stability number can be written:

$$N_s = \frac{H}{\Delta D_{n50}} < f(K, p_1, p_2, \dots, p_n) \quad (1)$$

where:

- H is a characteristic wave height of the incident sea state;
- Δ is the submerged density of the armour layer material;
- D_{n50} is the median nominal diameter of the armour layer units;
- p_1 to p_n are dimensionless parameters associated with the $n+3$ physical quantities considered in the tests
- K is an experimentally determined coefficient that reflects the influence of physical quantities not considered in the tests (Munson et al. 2009).

The most widely recognised empirical stability model was introduced by Hudson (1958), based on scale-model tests with regular, non-overtopping waves and armour layers composed of rock or tetrapod units:

$$N_s = (K_D \cot \alpha)^{1/3} \quad (2)$$

where α is the angle of the armour layer slope relative to the horizontal plan and K_D is the stability coefficient, a tabulated constant specific to each armour unit type and corresponding to a given percentage of damage at the end of the test. Damage in Hudson's formulation is defined by the volume of armour units displaced from the active zone of the breakwater, which extends from the mid-crest down the seaward slope to a depth approximately equal to the wave height.

Building on Hudson's formulation, Van der Meer (1985, 1988a) introduced a stability model for rock-armoured slopes that incorporates wave period effects through the Iribarren number (ξ_0), the number of waves (N_W), and core permeability (P):

$$N_s = 6.2 \xi_0^{-0.5} P^{0.18} \left(\frac{S}{\sqrt{N_W}} \right)^{0.2} \text{ for plunging waves} \quad (3)$$

$$N_s = 1.0 \xi_0^P \sqrt{\cot \alpha} P^{-0.13} \left(\frac{S}{\sqrt{N_W}} \right)^{0.2} \text{ for surging waves} \quad (4)$$

In both equations the dimensionless damage parameter, $S = A_e / (D_{n50})^2$ is used, where A_e is the eroded area of the profile and D_{n50} is the equivalent cube length.

Subsequently, Van der Meer (1988b) developed formulations applicable to cubes, tetrapods, and accropodes. Since the parameter S is not the most appropriate damage descriptor for these armour elements, Van der Meer adopted the parameter N_0 , defined as the number of units displaced from the armour layer within a strip of width equal to one equivalent cube length, following the approach originally proposed by Hedar (1960).

In 1999, Melby developed a damage evolution model based on long-duration laboratory tests to predict the progression of damage in a rock-armoured layer starting from an undamaged state ($S = 0$) at time $t = 0$, when exposed to constant wave conditions characterised by significant wave height H_s and mean period T_m .

$$S = a \left(\frac{H_s}{\Delta D_{n50}} \right)^5 \left(\frac{t}{T_m} \right)^b \quad (5)$$

In this expression, a and b are empirical parameters calibrated from scale-model test results. To extend the model to sequences of sea states with variable wave conditions, Melby and Kobayashi (1999) differentiated Eq. (5) with respect to time and integrated the result over a finite interval $t_n \leq t \leq t_{n+1}$, during which the wave parameters can be assumed constant (or characterised by spectral parameters H_{m0} and T_p):

$$S(t) = S(t_n) + a_p \left(\frac{H_{m0}}{\Delta D_{n50}} \right)^5 T_p^{-b} (t^b - t_n^b)$$

$$\text{for } t_n \leq t \leq t_{n+1} \quad (6)$$

This formulation allows for non-zero initial damage, with $S(t_n)$ representing the accumulated damage at time t_n . The coefficients a_p and b are empirical parameters obtained from experimental data. Based on scale-model tests of a rock-armoured rubble-mound breakwater, Melby (1999) proposed values of $a_p=0.0202$ and $b=0.25$.

Melby's experimental programme comprised three test series with peak wave periods of 2.48 s and 2.59 s and significant wave heights ranging from 0.098 m to 0.158 m. The longest series (Series A) aimed to verify damage stabilisation under successive sea states with constant characteristics. Each test condition, defined by a specific combination of wave height and period, was repeated until the number of displaced armour units remained unchanged in two consecutive tests. The programme then progressed to conditions with higher wave energy to assess long-term structural response.

Test Series B and C were of shorter duration. Series B examined increasing water levels and peak periods, whereas Series C investigated decreasing values of these parameters, with the aim of evaluating damage development under varying wave conditions.

The tested breakwater had a slope of 1:2 and an armour layer composed of rock units weighing 0.128 kgf (1.25 N), with a nominal diameter $D_{n50} = 0.034$ m. Damage assessment was performed using a mechanical profiler equipped with eight arms to survey individual cross-shore profiles. The damage parameter S for each test was computed as the average value obtained from the eight profiles. This approach becomes less reliable as the number of surveyed profiles decreases, whereas increasing the number of profiles covering the entire slope reduces associated uncertainties.

In comparison with the Van der Meer formulations (Eqs. 3 and 4), Melby's formulation (Eq. 5) does not include the Iribarren number. Consequently, the slope of the armour layer is not explicitly accounted for, and the empirical coefficients a_p and b must be recalibrated to represent damage evolution for different slopes and armour types. Furthermore, when armour units other than rock are employed, coefficients calibrated for rock armour layers are not directly applicable.

As a first step towards adapting Melby's coefficients to armour layers composed of units other than rock, a procedure based on the derivation of Eq. (6) presented in Melby (1999) was adopted. Within the time interval $t_n \leq t \leq t_{n+1}$, assuming constant wave conditions, the following expressions can be written:

$$S_{n+1} = a_p \left(\frac{H_{m0}}{\Delta D_n} \right)^5 \left(\frac{t_{n+1}}{T_p} \right)^b \quad (7)$$

$$S_n = a_p \left(\frac{H_{m0}}{\Delta D_n} \right)^5 \left(\frac{t_n}{T_p} \right)^b \quad (8)$$

Dividing S_{n+1} by S_n and applying logarithms to calculate b yields:

$$b = \frac{\ln\left(\frac{S_{n+1}}{S_n}\right)}{\ln\left(\frac{t_{n+1}}{t_n}\right)} \quad (9)$$

In terms of Melby's expression, the coefficient a_p can then be determined as:

$$a_p = \frac{S_{n+1} - S_n}{\left(\frac{H_{m0}}{\Delta D_n} \right)^5 \left[\left(\frac{t_{n+1}}{T_p} \right)^b - \left(\frac{t_n}{T_p} \right)^b \right]} \quad (10)$$

For tests conducted under similar wave conditions, the estimated values of b and a_p should exhibit limited variability. Averaging the values obtained across all test conditions provides an initial estimate of the coefficients for the tested structure. Subsequently, the optimal values of a_p and b can be determined by minimising the root mean square error between measured and predicted damage.

The present study focuses on recalibrating these empirical coefficients to improve damage evolution predictions for breakwaters armoured with tetrapods. In particular, the coefficients previously adjusted by Lemos et al. (2023) are validated and refined under wave conditions influenced by bathymetry, using experimental data from three-dimensional surveys of the Ericeira breakwater, which serves as a representative case study for similar coastal structures.

2.2 Case study: Ericeira breakwater

The Ericeira breakwater, constructed in the 1970s, is located on the western coast of Portugal and serves as a key coastal defence structure, protecting the town's harbour from Atlantic wave action and storm events (Fig. 2). Situated in a region renowned for fishing and surfing activities, Ericeira relies on the breakwater to safeguard both critical infrastructure and maritime operations.

Over the years, the structure has undergone several major repair interventions, particularly following severe storm events in the 1990s, 2001, 2007, 2013, and 2018. These rehabilitation works included the replacement of displaced armour units, replenishment of core materials, and reinforcement of the breakwater to improve resistance to future wave impacts. Continuous

maintenance remains essential to ensure the long-term effectiveness of the structure in harbour protection.

2.3 Experimental set-up and test conditions

The experimental study was carried out at the Ports and Maritime Structures Unit (NPE) of the Hydraulics and Environment Department of the National Laboratory for Civil Engineering (LNEC), in Lisbon, Portugal. Experiments were conducted in a wave basin measuring 46.6 m in length, 20.6 m in width, and 1.5 m in depth, equipped with a piston-type wave generation system. The physical model represents the port basin up to the harbour entrance (Fig. 2).

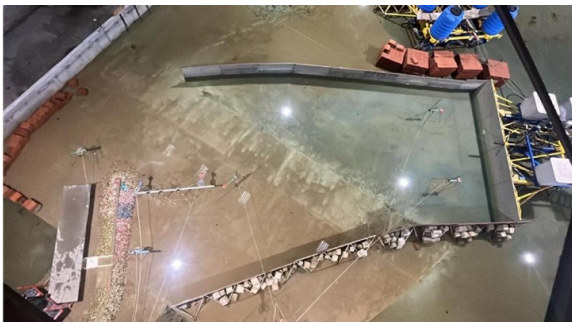


Figure 2. Physical model of the Ericeira breakwater.

The model was constructed and operated at a geometric scale of 1:65, following Froude similarity. The tested breakwater has a 2:3 slope and a two-layer rock filter covering the core. The armour layer of the breakwater sections (Fig. 3a) is composed of:

- Trunk: 300 kN tetrapods with a nominal diameter of 0.034 m and a porosity of 0.45;
- Head: 550 kN Antifer cubes with a nominal diameter of 0.042 m and a porosity of 0.30.

The selected scale of 1:65 reflects a compromise between the dimensions of the experimental facility and the spatial extent of the coastal area of interest.

Dissipative beaches were installed along the basin sidewalls to minimise unwanted wave reflections.

The experimental instrumentation included eight resistive wave gauges (Fig. 3b) used to measure free-surface elevation. A Kinect position sensor was employed to survey the armour layer geometry at the beginning of the test programme and after each individual test, allowing detailed assessment of damage evolution.

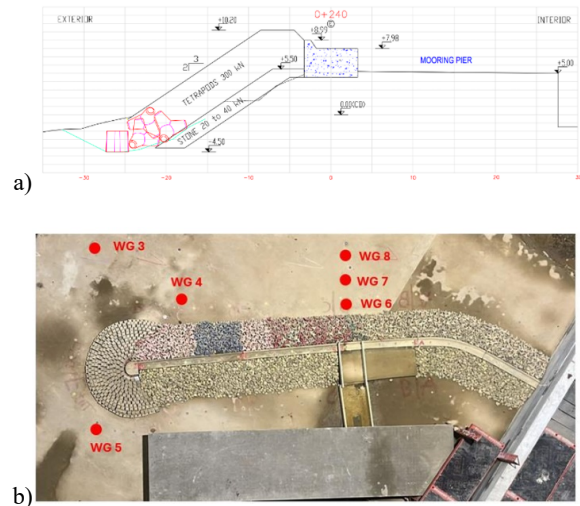


Figure 3. a) Trunk cross-section. b) three-dimensional scale model and wave gauge locations

2.4 Wave conditions

The tested wave conditions were defined based on hindcast data and buoy measurements. They correspond to peak wave periods of $T_p = 14$ s and $T_p = 16$ s, associated with High Water Level (HWL) and High Water Level with set-up (HWLS), respectively. Significant wave heights of $H_s = 5$, 6, and 7 m were considered, with a north-westerly (NW) wave direction, corresponding to an almost frontal wave attack on the breakwater (Fig. 4).

These conditions encompass the expected range of sea states acting on the structure, including extreme events and potential effects of climate change on wave characteristics and water levels.

Three test series were conducted in the experimental programme (Table 1). Test Series A, with a duration of 30 hours (model scale), was designed to provide insight into the long-term deterioration of the structure, up to near-failure conditions.

Given the characteristics of the armour layer units (tetrapods), their interlocking capacity, and the durability required throughout the structure's service life—particularly before emergency intervention becomes necessary—the tests were extended slightly beyond the failure threshold defined by Melby and Kobayashi (1998). In their study, failure was defined as exposure of the underlayer through a hole with a diameter of at least D_{n50} . In the present study, the adopted criterion lies between the Initiation of Damage and Destruction, as defined by Losada et al. (1986) and Vidal et al. (1991).

In Test Series A, testing was interrupted when the analysed section of the breakwater approached a

condition in which it no longer complied with its required level of service. At the end of this series, approximately four to five armour units from the lower layer had been displaced, and the underlayer was partially exposed to wave action.

Table 1. Water levels and wave conditions for test series A, B, and C (model scale values)

| Series | Test | T_p (s) | Hm0 (m) | Depth at the toe (m) | Number of test runs |
|--------|------|-----------|---------|----------------------|----------------------------|
| A | 1 | 1.74 | 0.08 | 0.14 | Until damage stabilisation |
| | 2 | 1.74 | 0.09 | 0.14 | |
| | 3 | 1.74 | 0.10 | 0.14 | |
| | 4 | 1.99 | 0.09 | 0.17 | |
| | 5 | 1.99 | 0.10 | 0.17 | |
| B | 1 | 1.74 | 0.08 | 0.14 | 1 |
| | 2 | 1.74 | 0.09 | 0.14 | 4 |
| | 3 | 1.74 | 0.10 | 0.14 | 4 |
| | 4 | 1.99 | 0.09 | 0.17 | 4 |
| | 5 | 1.99 | 0.10 | 0.17 | 2 |
| C | 4 | 1.99 | 0.09 | 0.17 | 4 |
| | 5 | 1.99 | 0.10 | 0.17 | 2 |
| | 1 | 1.99 | 0.08 | 0.14 | 4 |
| | 2 | 1.74 | 0.09 | 0.14 | 4 |
| | 3 | 1.74 | 0.10 | 0.14 | 4 |

The model structure was exposed sequentially to wave conditions 1 to 5 until damage stabilisation was observed. Wave conditions 1 to 3 correspond to HWL, whereas conditions 4 and 5 correspond to HWLS. In both cases, wave height increased progressively from condition 1 to 3 and from condition 4 to 5. Transitions between wave conditions were implemented once the damaged armour profile exhibited stabilisation.

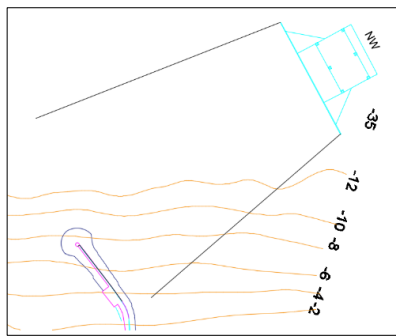


Figure 4. Detail of the three-dimensional model installation in the wave basin, including bathymetry.

2.5 Methodology for damage evolution quantification

In the present study, the dimensionless damage parameter, $S = Ae/D_n^2$ was adopted, where A_e represents the eroded area of the armour profile and D_n denotes the nominal diameter of the tetrapod units. The parameter S may be interpreted as the number of squares with side length D_{n50} required to cover the eroded area.

Recent advances in three-dimensional survey techniques, including LiDAR, photogrammetry, and artificial vision algorithms, have enabled the

combined use of multiple damage descriptors. Given the complexity of defining representative surface profiles for tetrapod armour layers, damage parameters based solely on two-dimensional profiles are less suitable. To overcome this limitation, the mean eroded area was computed from the total eroded volume of the armour layer.

Specifically, the section-averaged eroded area (A_e) was obtained by dividing the eroded volume (E_v) measured at the end of each test by the width of the analysed stretch (X).

The dimensionless damage parameter S was subsequently calculated from this averaged eroded area. To minimise errors associated with spatial averaging, the analysis was restricted to the zone exhibiting the highest damage concentration.

Damage assessment was based on eroded volume measurements derived from surveys performed using a Kinect V2 position sensor. The sensor was mounted on a tripod and positioned approximately 2 m from the crest of the structure (Fig. 5a). The survey parameters included a voxel resolution of 512 points along each of the three spatial axes (x, y, z), corresponding to 256 voxels per metre. As a result, each scanned scene covered a volume of 2 m \times 2 m \times 2 m. The effective acquisition range of the sensor was between 0.5 m and 8 m.

Kinect surveys were carried out without water in the wave tank at the beginning of the test programme and at the end of each test series, and with water in the tank at the end of each intermediate test. In addition, traditional visual counting of rocking and displaced armour units was performed, when possible, to support calibration of the grid resolution used during point-cloud post-processing.

To reference the point clouds obtained from the Kinect surveys—i.e. to transform coordinates from the sensor reference frame to a coordinate system fixed to the flume bottom—70 ground control points (GCPs) were employed. These GCPs consisted of coloured markers placed on the flume bottom in front of the toe of the structure and on the superstructure (Fig. 5b). Their coordinates were measured using a total station prior to the start of the experimental programme.



Figure 5. (a) Kinect position sensor; (b) ground control points

This referencing procedure also facilitates correction of distortions caused by light refraction at the air–water interface during surveys conducted with water in the tank. Such refraction correction is only possible when submerged GCPs are detected by the sensor, enabling correction of rotational misalignment. A similar approach was adopted by Musumeci et al. (2018) in their Kinect-based surveys of scale-model rubble-mound breakwaters.

Post-processing of the surveys conducted with water in the flume also included a fine alignment of the resulting point clouds with reference clouds obtained without water. This alignment was performed using the iterative closest point (ICP) algorithm (Chen et al., 1992), implemented in the open-source software CloudCompare (Girardeau-Montaut, 2006). For each point in the cloud obtained with water, the ICP algorithm identifies the closest corresponding point in the reference cloud and estimates the optimal combination of rotation and translation that minimises the root mean square (RMS) point-to-point distance.

The algorithm iterates until a stopping criterion is met, defined either by an RMS threshold or a maximum number of iterations. In the present study, an RMS tolerance of 10^{-5} m was adopted, corresponding to a near-complete final overlap, as recommended by the software.

Eroded volume computation was based on gridding of the point clouds, which defines the size of the elementary cells used in volume estimation. CloudCompare computes the eroded volume by summing the volumes of elementary parallelepipeds whose base area corresponds to the grid cell area and whose height equals the vertical difference between corresponding points in the two clouds ($dV = \text{grid step} * \text{grid step} * \text{distance}$).

Prior to final volume computation, calibration of the grid size was performed using tests involving the removal of a small number of armour units. This procedure aimed to identify a grid resolution yielding eroded volume estimates consistent with visually counted displaced units. After testing grid steps ranging from 1.0 mm to 2.0 mm, an optimal grid size of 1.4 mm was selected,

providing the best compromise between point density and depth resolution.

The novelty of the present damage evaluation methodology lies in the use of three-dimensional surface models of the armour layer to compute eroded volume from differences between successive surveys and, from this, derive the eroded area (A_e) and the dimensionless damage parameter S . In this study, A_e was obtained by dividing the total eroded volume by the length of the analysed stretch. This simplification is justified for structure sections where damage is spatially homogeneous, as in the present case. Although damage parameters could alternatively be derived from individual profiles extracted from the point clouds, the homogeneous nature of damage observed in the study area motivated the use of a volume-based approach rather than profile-based estimates.

Interactions among individual concrete armour units under breaking wave action are highly complex (Xiang et al., 2022). Consequently, the use of eroded volume and area as proxies for damage may introduce uncertainties in the calculation of S . Accurate knowledge of armour layer porosity—particularly at the beginning of the test programme—and careful calibration of the grid resolution are therefore essential to minimise potential over- or underestimation of the damage parameter.

3 RESULTS AND DISCUSSION

The results presented in this section refer to test series A and B. Test series C is currently under analysis. Table 2 summarises the number of tests performed for each test series.

Damage evaluation in this study focuses on the most severely affected zone of the breakwater, corresponding to a stretch of the trunk located near the head of the structure. Owing to wave transformation induced by the local bathymetry, this area experienced the highest damage levels. The analysed stretch had a width X of 0.53 m for test series A and 0.64 m for test series B (Fig. 6 **Errore. L'origine riferimento non è stata trovata.**).

Table 2. Number of tests for each test series

| Series | Test | Test repeats until stabilization | Test names |
|--------|------|----------------------------------|------------|
| A | 1 | 3 | T1-T3 |
| | 2 | 19 | T4-T22 |
| | 3 | 26 | T23-T45 |
| | 4 | 7 | T46-T52 |
| | 5 | 2 | T53-T54 |
| B | 1 | 1 | T1 |
| | 2 | 4 | T2-T5 |

| | | | |
|---|---|---|---------|
| B | 3 | 4 | T6-T9 |
| | 4 | 4 | T10-T13 |
| | 5 | 2 | T14-T15 |

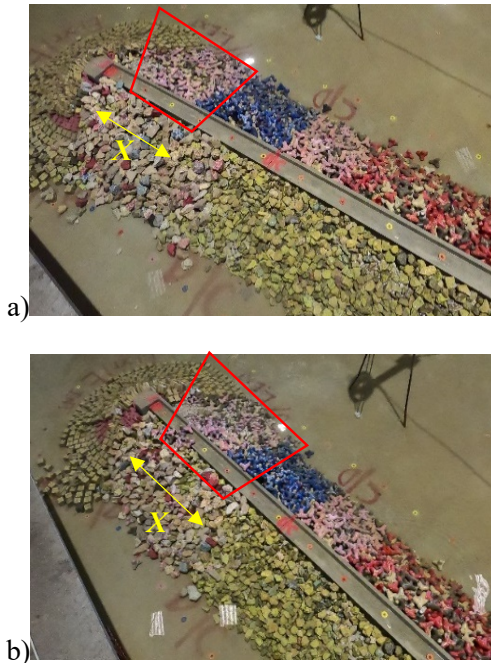


Figure 6. Overview of the model at the end of test series A (a) and B (b)

It should be noted that the eroded area represents an average value; individual profiles may exhibit variability due to the spatial heterogeneity of damage distribution. Figures 7 and 8 present the point clouds obtained from Kinect© sensor surveys conducted at the beginning and end of test series A (T3, T22, T45, and T54) and test series B (T4, T8, T12, and T15), respectively. Corresponding distance maps between the initial and final surveys are also shown.

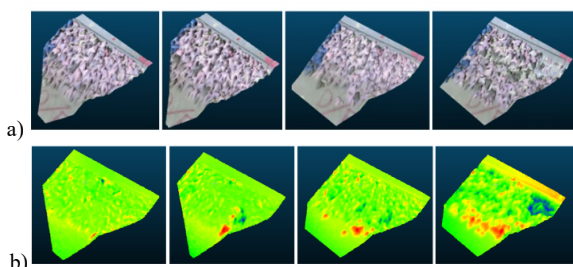


Figure 7. Surveys for tests T3, T22, T45, and T54 of test series A: (a) point clouds; (b) distance map (blue: erosion; red: deposition)

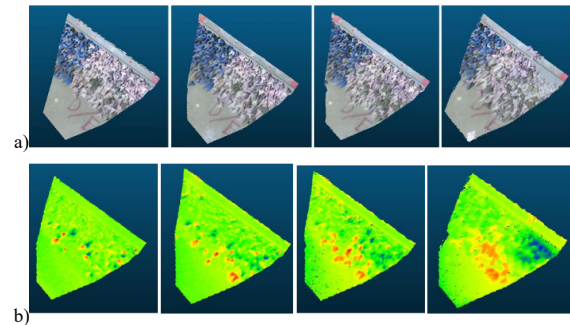


Figure 8. Surveys for tests T4, T8, T12, and T15 of test series B: (a) point clouds; (b) distance map (blue: erosion; red: deposition)

For test series A (Fig. 9a), damage progression increased with rising water levels and peak wave periods. At the end of the high-water level (HWL) tests, and according to the qualitative damage thresholds defined by Losada et al. (1986) and Vidal et al. (1991), the damage level remained within the *Damage Initiation* category. However, following the high-water level with set-up (HWLS) tests, the damage escalated to the *Destruction* category.

In test series B, damage evolved more gradually, influenced by both water level and peak period, and increased with significant wave height (Fig. 9b). At the end of the HWL tests, the damage corresponded to the *Iribarren damage* classification, characterised by significant exposure of the lower tetrapod layer. As in test series A, the HWLS tests led to damage reaching the *Destruction* category. In both test series, damage was predominantly concentrated in the upper portion of the armour layer.

Figure 11 compares measured and predicted values of the dimensionless damage parameter S , using coefficients $a_p = 0.03$ and $b = 0.16$ proposed by Lemos et al. (2023) for test series A. These coefficients were derived from two-dimensional scale model tests with similar prototype wave conditions and identical cross-sectional geometry.

As expected, results from the three-dimensional physical model do not converge with those obtained from the two-dimensional formulation. Predicted values consistently underestimate the measured damage, particularly towards the end of the test programme. This discrepancy is primarily attributed to:

- (a) three-dimensional effects associated with bathymetric reproduction in the physical model; and
- (b) differences in armour unit scaling and stability.

The 2D model was conducted at a 1:50 scale, with armour units equivalent to 105 kN in the prototype, deliberately resulting in a less stable armour layer. In contrast, the 3D model was built at a 1:65 scale, with armour units corresponding to their actual prototype weight (300 kN). This led to lower stability numbers and higher damage progression in the 3D model.

To recalibrate the Melby damage evolution coefficients for three-dimensional conditions, constant sea-wave conditions at the structure toe were defined using average values of peak period and significant wave height for each test sequence.

Table 3 summarises the start and end times of each sequence, corresponding damage values, and averaged wave characteristics.

Table 3. Average sea-wave characteristics at the toe of the structure and corresponding damage parameters

| Test series A | | | | | | | |
|---------------|--------|---------|--------|------|----------|------|------|
| Test | Tp (s) | Hm0 (m) | tn (s) | Sn | tn+1 (s) | Sn+1 | Nm0 |
| 1 | 1.67 | 0.05 | 0 | 0 | 5208 | 0.6 | 0.85 |
| 2 | 1.69 | 0.08 | 5208 | 0.5 | 38192 | 0.9 | 1.30 |
| 3 | 1.73 | 0.10 | 38192 | 0.8 | 78120 | 1.2 | 1.57 |
| 4 | 1.63 | 0.07 | 80105 | 1.6 | 92015 | 2.6 | 1.14 |
| 5 | 1.59 | 0.09 | 92015 | 3 | 99955 | 3.9 | 1.45 |
| Test series B | | | | | | | |
| Test | Tp (s) | Hm0 (m) | tn (s) | Sn | tn+1 (s) | Sn+1 | Nm0 |
| 1 | 1.73 | 0.07 | 0 | 0 | 1736 | 0.5 | 1.13 |
| 2 | 1.72 | 0.09 | 1736 | 0.50 | 8680 | 0.8 | 1.46 |
| 3 | 1.73 | 0.10 | 8680 | 0.80 | 15624 | 1.5 | 1.59 |
| 4 | 1.75 | 0.08 | 15624 | 1.50 | 23564 | 2.4 | 1.22 |
| 5 | 1.75 | 0.09 | 23564 | 2.40 | 27534 | 3.9 | 1.44 |

By minimising the root mean square error (RMSE) between measured and predicted damage values over various combinations of a_p and b , optimal coefficients were identified within the range defined by the standard deviation of the measured S values (Fig. 9). The standard deviation was computed using all measured damage values obtained at the end of each test run.

An initial optimisation yielded coefficients $a_p = 0.03$ and $b = 0.27$ for test series A, corresponding to an RMSE of 0.7. Despite this adjustment, the predicted damage trend did not fully reproduce the measured progression.

Analysis of Fig. 9a shows that, during HWL conditions, predicted damage values match

measured values reasonably well up to approximately 25,000 waves. Beyond this point, and until the end of the HWL tests (around 45,000 waves), the formulation tends to overestimate the stabilised measured damage. When transitioning to HWLS conditions, the predicted curve fails to capture the abrupt increase in measured damage, resulting in underestimation.

This rapid damage escalation is likely related to increased wave run-up and rundown caused by higher water levels and longer wave periods, leading to energy concentration in the upper part of the slope—where damage was most localised. Such effects are not explicitly accounted for in the formulation and contribute to faster damage evolution than predicted.

Although the formulation was originally intended for life-cycle cost forecasting and not expected to exceed the *Initiation of Destruction* level, the rapid damage progression observed is representative of the Ericeira breakwater case. Consequently, the authors deemed it necessary to further adjust the coefficients to account for rapid damage evolution.

To capture this behaviour, RMSE minimisation was performed separately for HWL and HWLS conditions, maintaining $a_p = 0.03$. The final coefficients obtained were:

- HWL: $a_p = 0.03$, $b = 0.27$ (RMSE = 0.33);
- HWLS: $a_p = 0.03$, $b = 0.47$ (RMSE = 2.5).

The recalibrated coefficients provide a reasonable agreement between predicted and measured damage values for test series A (Fig. 9b).

Validation using test series B confirmed the applicability of the proposed coefficients. As shown in Fig. 10, predicted damage values exhibit reasonable agreement with measured data, with RMSE values of 1.7 for HWL and 4.18 for HWLS.

Regarding damage initiation, the formulation underestimates damage in test series A but performs satisfactorily for test series B.

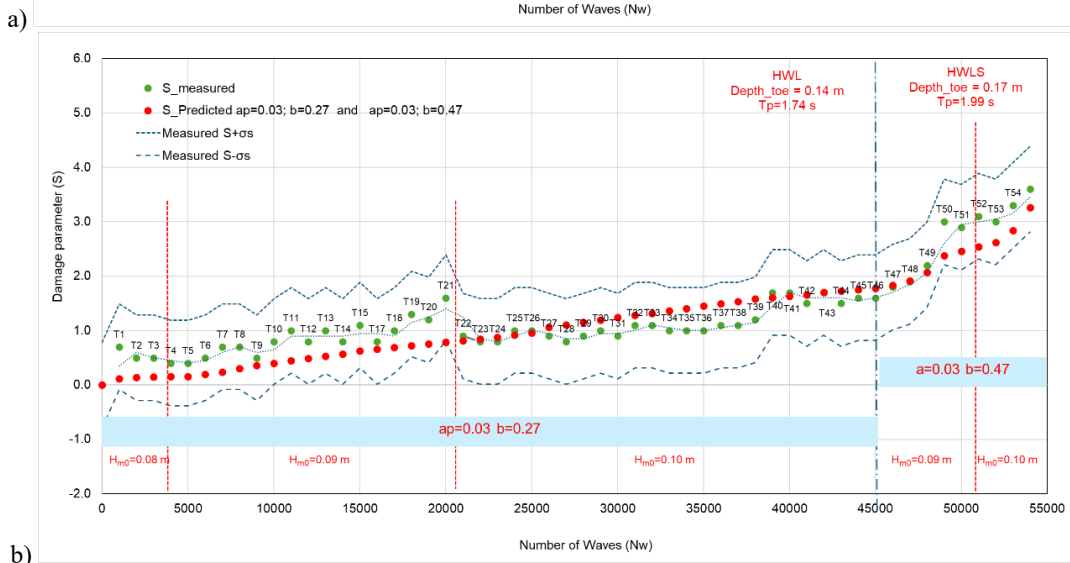
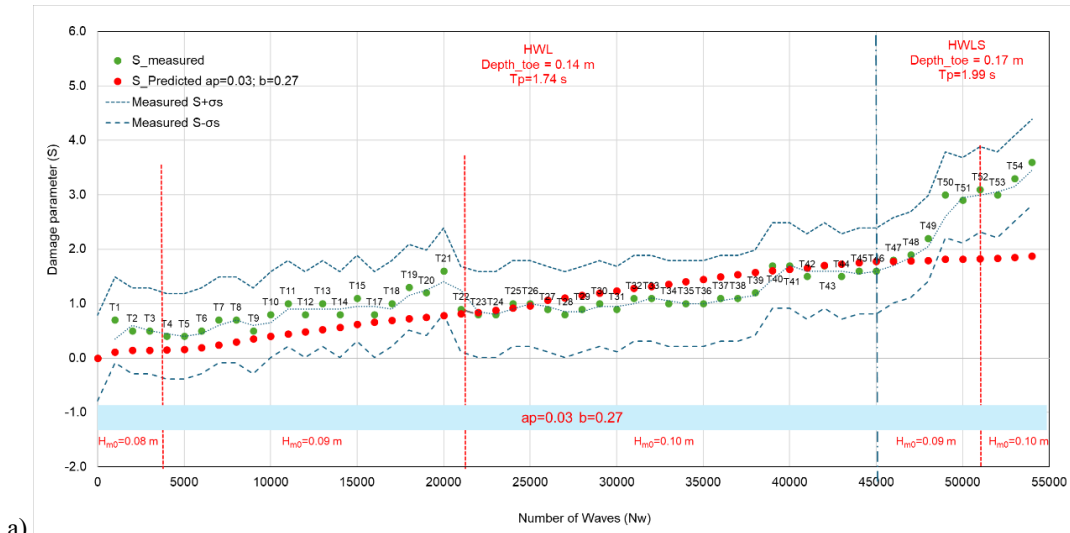


Figure 9. Measured and predicted damage parameter (S) with fitted a_p and b parameters for test series A a) using the same a_p and b parameters for tests with HWL and HWLS b) using readjusted b parameter for tests with HWLS

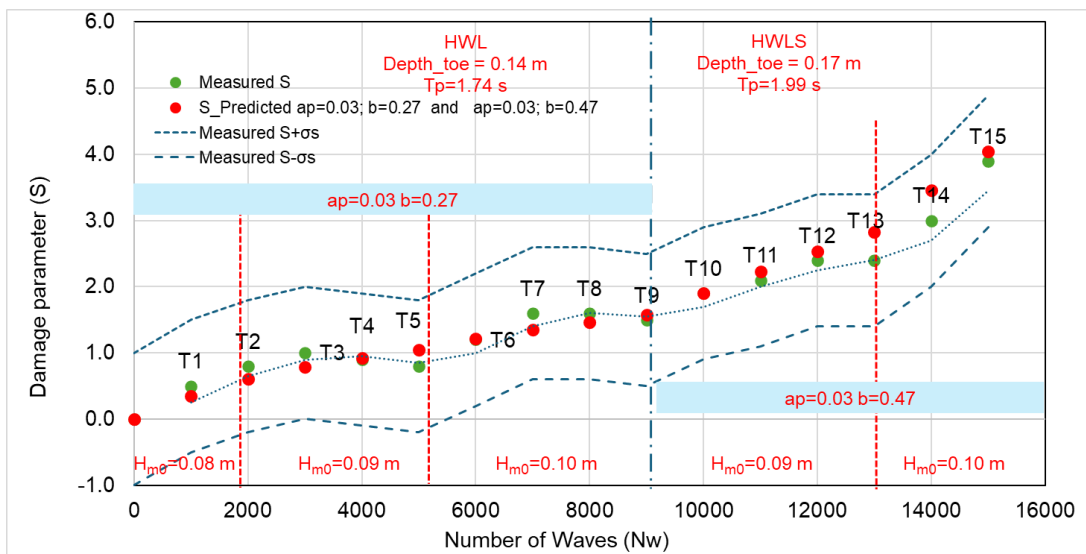


Figure 10. Measured and predicted damage parameter (S) for test series B using readjusted a_p and b parameters

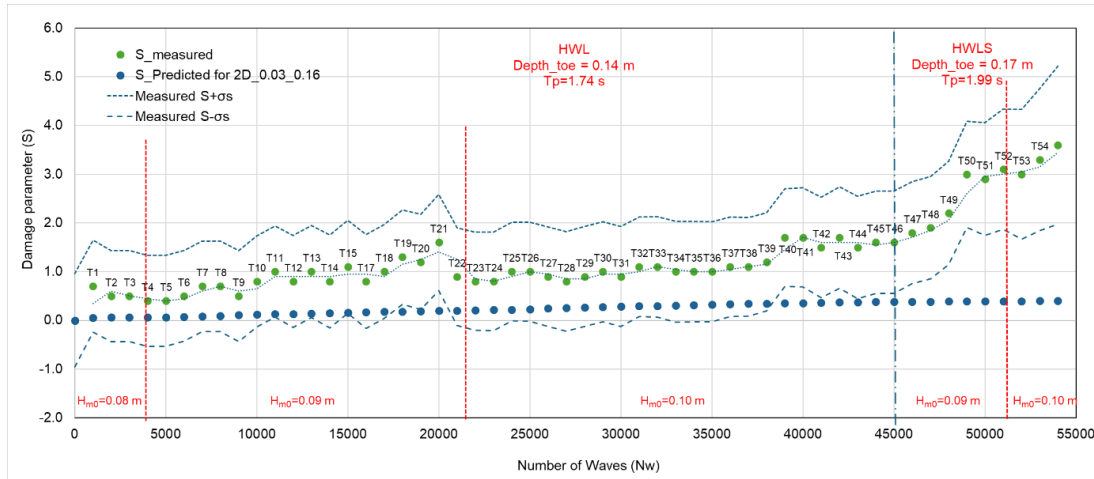


Figure 11. Measured and predicted damage parameter (S) with a_b and b parameters from Lemos et al, 2023

The Melby and Kobayashi predictive model assumes a continuously increasing damage progression at a decreasing rate. In theory, prolonged exposure to small waves between storms may contribute to incremental damage. This behaviour was observed in both test series; however, in test series A, an abrupt increase in damage occurred at the onset of HWL conditions.

Overall, the Melby and Kobayashi (1988a,b) formulation, fitted for the present test programme, armour layer type, and bathymetric influence, with coefficients $a_p = 0.03$ and $b = 0.27$, adequately describes damage evolution for the relatively low damage levels observed under HWL conditions. For higher damage levels under HWLS conditions, the coefficients $a_p = 0.03$ and $b = 0.47$ also provide a reasonable representation of damage trends, despite the associated increase in RMSE.

4 CONCLUSIONS

The present work revisits the damage evolution formulations proposed by Melby and Kobayashi, with the aim of establishing an equivalent formulation for the armour layer damage evolution of rubble-mound breakwaters protected by tetrapods. An initial approach was previously developed using a two-dimensional scale model of a section of the Ericeira breakwater (Lemos et al., 2023). In the present study, those coefficients were further refined by explicitly accounting for three-dimensional effects on damage progression, through three sets of three-dimensional physical model tests.

The characterisation of armour layer damage was based on surveys performed using a position sensor. The use of this sensor proved to be effective in generating three-dimensional surface models of the armour layer, enabling the quantification of damage indicators such as eroded volume and mean eroded area. Although the interaction between individual armour units was not explicitly considered—an inherent simplification that may influence the calculation of the damage parameter S —the adopted methodology provided consistent and reliable damage estimates.

The Melby and Kobayashi (1988a, 1988b) formulation, when recalibrated with the updated coefficients $a_p = 0.03$ and $b = 0.27$, was found to describe the damage evolution satisfactorily for relatively low damage levels, with predictions lying within one standard deviation of the measured values. For higher damage levels, the coefficients $a_p = 0.03$ and $b = 0.47$ were shown to capture the overall trend of damage evolution reasonably well, albeit with an increase in the root mean square error (RMSE).

The study demonstrates that long-duration tests can represent a valuable extension of conventional hydraulic stability tests conducted in wave flumes or wave basins, which are typically focused on assessing the behaviour of a proposed rubble-mound breakwater cross-section under design conditions. Using the same experimental setup, the procedure presented herein enables the derivation of the empirical coefficients a_p and b governing armour layer damage evolution.

Once these coefficients are calibrated and combined with knowledge of the local wave

climate at the site of interest, the proposed methodology allows the forecasting of future armour layer damage evolution over the time interval following the most recent periodic inspection. This capability provides a useful tool for supporting maintenance planning and long-term performance assessment of rubble-mound breakwaters protected with concrete armour units.

ACKNOWLEDGEMENTS

This work was supported by the Instituto Superior de Educação e Ciências (ISEC-Lisboa) through the project ProCoast 3D/CPISEC/PID/001/2023-24, within the framework of the COASTLIFE project financed by the Fundação para a Ciência e a Tecnologia (FCT). Additional support was provided by the projects SAFEPOR and WISER, developed within the scope of the *Risk and Safety in Ports and Maritime Structures* Programme of the Research and Innovation Strategy (E2I) 2021–2027 of LNEC

REFERENCES

- Broderick, L. (1983). *Riprap Stability*, a Progress Report. In *Coast. Struct.*; ASCE: Reston, VA, USA, 1983; pp. 320–330
- Burcharth, H.F.; Hughes, S.A. (2011). *Fundamentals of Design*. In *Coastal Engineering Manual*; USACE Publications: Hyattsville, MD, USA.
- Campos, A.; Castillo, C.; Molina-Sanchez, R. (2020). Damage in Rubble Mound Breakwaters. Part I: Historical Review of Damage Models. *J. Mar. Sci. Eng.* 2020, 8, 317.
- Chen, Y.; Medioni, G. (1992). Object modelling by registration of multiple range images. *Image and vision computing*, 10.3: 145-155.
- Girardeau-Montaut, D. (2006). *Détection de changement sur des données géométriques tridimensionnelles*. PhD Thesis. Télécom ParisTech.
- Hedar, P.A. *Stability of Rock-Fill Breakwaters* (1960). Ph.D. Thesis, University of Gothenburg, Gothenburg, Sweden.
- Hudson, R.Y. (1958). *Design of Quarry-Stone Cover Layers for Rubble-Mound Breakwaters*; WES: Vicksburg, MS, USA.
- Lemos R., Santos J.A., Fortes C.J.E.M. (2023). Damage Evolution Prediction during 2D Scale-Model Tests of a Rubble-Mound Breakwater: A Case Study of Ericeira's Breakwater. *Modelling* 2023 4, 1–17. <https://doi.org/10.3390/modelling4010001>
- Losada, M.A.; Desire, J.M.; Alejo, L.M. (1986). Stability of Blocks as Breakwater Armor Units. *J. Struct. Eng.* 112, 2392–2401.
- Melby, J.; Kobayashi, N. (1998a). Progression and Variability of Damage on Rubble Mound Breakwaters. *J. Waterw. Port., Coastal, Ocean. Eng.* 124, 286–294
- Melby, J.A.; Kobayashi, N. (1998b). Damage Progression on Breakwaters. In *Proceedings of the 26th International Conference on Coastal Engineering*, Copenhagen, Denmark, 22–26 June 1998; Volume 2, pp. 1884–1897.
- Melby, J.A.; Kobayashi, N. (1999). Damage Progression and Variability on Breakwater Trunks. In *Proceedings of the Coastal Structures*, Santander, Spain, 7–10 June 1999; Volume 1, pp. 309–315.
- Melby, J.A. (1999). *Damage Progression on Rubble-Mound Breakwaters*; US Army Corps of Engineers: Washington, DC, USA.
- Munson, B.R.; Young, D.F.; Okiishi, T.H.; Huebsch, W.W (2009). *Fundamentals of Fluid Mechanics*, 6th ed.; John Wiley & Son, Inc.: Hoboken, NJ, USA.
- Musumeci, R.; Moltisanti, D.; Foti, E.; Battiato, S. (2018). 3-D monitoring of rubble-mound breakwater damages. *Measurement*, 117, 347–364.
- United States Army Corps of Engineers (2011). *Coastal Engineering Manual*, USACE: Washington, DC, USA
- van der Meer, J.W. (1985). Stability of Rubble Mound Revetments and Breakwaters under Random Wave Attack. In *Proceedings of the Breakwaters Conference*, London, UK, 2–4 October 1985.
- van der Meer, J.W. (1988a). *Rock Slopes and Gravel Beaches under Wave Attack*. Ph.D. Thesis, Faculty of Civil Engineering and Geo-sciences, Delft, The Netherlands, 26 April 1988.
- van der Meer J.W. (1988b). Stability of Cubes, Tetrapodes and Accropode. In *Proceedings of the Breakwaters Conference*, Eastbourne, UK, 2–4 May 1988; pp. 71–80
- Vidal, C.; Losada, M.; Medina, R. (1991). Stability of Mound Breakwater's Head and Trunk. *J. Waterw. Port Coast. Ocean Eng.*, 117, 570–587.
- Xiang, J., Latham, J.-P. and Higuera, P. (2022). Numerical study of Core-Loc™ breakwater stability under storm wave sea state using a fast wave proxy approach. *COSE*, Year 1, Volume 2, 6-18.
- Yuksel, Z. T., & Kobayashi, N. (2022). Numerical modeling of revetment and sill in reducing shore erosion. *COSE*, Year 1, Volume 1, 8-19.